Stable solitons in elliptical photonic lattices

Adrian Ruelas, Servando Lopez-Aguayo,* and Julio C. Gutiérrez-Vega

Photonics and Mathematical Optics Group, Tecnológico de Monterrey, Monterrey, México 64849
**Corresponding author: servando@itesm.mx*

Received August 4, 2008; revised October 13, 2008; accepted October 17, 2008; posted October 20, 2008 (Doc. ID 99746); published November 21, 2008

We introduce the basic properties of solitons in elliptical photonic lattices induced optically by a superposition of Mathieu beams. Owing to the modulation of the intensity along its elliptical rings, these lattices allow novel dynamics of propagation, being possible, for the first time to our knowledge, to propagate solitons in an elliptic motion with varying rotation rate. © 2008 Optical Society of America

OCIS codes: 190.4360, 190.4420, 190.6135.

The combination of diffractive and nonlinear effects with the depth of the transverse refractive index modulation in photonic lattices opens the possibility to produce spatial localized states of light—or solitons—in either weak or strong coupling regimes [1–5]. This tunable discreteness offers a rich variety of phenomena that are not possible to observe in homogeneous media. To achieve a maximum control of light in these media, the lattice itself must minimize the diffraction effects, and therefore the nondiffracting beams [6] are appropriate to induce the photonic lattice. The simplest case of a nondiffracting beam are the plane waves, which are the fundamental solution to the Helmholtz equation in Cartesian coordinates. Over the past few years, more complex nondiffracting beams solutions, such as Bessel, Mathieu, and parabolic beams in circular, elliptical, and parabolic coordinate systems, respectively, have been analyzed both in linear [6–8] and nonlinear [9–12] materials. The properties of the solitons supported by the optical lattice change substantially as a result of the topology and symmetries of the nondiffracting beam employed. In a past work, the basic properties and stability of two-dimensional solitons in optical lattices induced by the pure even and odd Mathieu beams were addressed [11].

In this Letter we introduce a new topology of optical lattice: the elliptical photonic lattice (EPL). Such a lattice is induced optically by a linear superposition of Mathieu nondiffracting beams [13]. We reveal that single solitons can be set into elliptic rotation with varying angular velocity by adjusting the depth and ellipticity of the lattice and the initial power and transverse momentum of the solitons. Remarkably, the rotating solitons can propagate without power radiation for several tens of diffraction lengths and rotations. To the best of our knowledge, the EPL is the first lattice where all these properties are present at the same time. This Letter consolidates and extends previous studies on Bessel and lowest-order Mathieu lattices [9,11].

We begin the analysis by writing the nonlinear propagation equation for the complex field amplitude Ψ, traveling along the z axis of a self-focusing saturable medium whose refractive index varies transversely as $\Gamma(\mathbf{r})$

$$i\frac{\partial\Psi}{\partial z} = -\left(\frac{\partial^2}{\partial x^2}+\frac{\partial^2}{\partial y^2}\right)\Psi - \frac{|\Psi|^2}{1+s|\Psi|^2}\Psi - p\Gamma(\mathbf{r})\Psi, \quad (1)$$

where the longitudinal z and the transverse coordinates $\mathbf{r}=(x,y)$ have been normalized to the diffraction length and the beam width, respectively; p is the lattice depth; and s is the saturation parameter [14]. We assume that the EPL is described by the transverse intensity $\Gamma(\mathbf{r})\sim|\tau(\mathbf{r})|^2$ of a nondiffracting helical Mathieu beam [7,13], namely,

$$\tau(\mathbf{r}) = \int_0^{2\pi} [\mathcal{C}\mathrm{ce}_m(\phi;\epsilon) + i\mathcal{S}\mathrm{se}_m(\phi;\epsilon)] \times \exp[ik_t(x\cos\phi + y\sin\phi)]\mathrm{d}\phi, \quad (2)$$

where ce_m and se_m are the mth-order even and odd Mathieu functions, $\mathcal{C}(\epsilon)$ and $\mathcal{S}(\epsilon)$ are normalization constants to ensure that the even and odd components carry the same power, $\epsilon\in[0,\infty)$ is the ellipticity parameter, and k_t is the transverse wave vector. As shown in Fig. 1 , the transverse index distribution of the EPL is characterized by a set of confocal elliptic rings whose ellipticity is controlled by ϵ. When $\epsilon\to 0$ the EPL reduces to a Bessel lattice characterized by a set of circular rings of constant intensity [9]. As ϵ increases, the rings become more and more elliptical and, after a critical value of ϵ, they are broken. When $\epsilon\to\infty$, the EPL tends smoothly to a discrete rectangu-

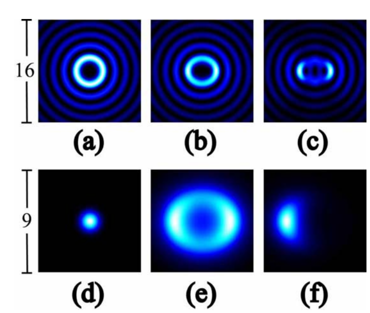

Fig. 1. (Color online) Transverse profile of third-order EPLs with $k_t=2$ for (a) $\epsilon=0$, (b) $\epsilon=1$, and (c) $\epsilon=2$. Profiles of centered solitons supported by a third-order EPL with $s=0.05$, $\epsilon=1$, $k_t=2$, and $p=2$ for (d) $\beta=0.8$, (e) $\beta=15$, and (f) $\beta=20$.

lar lattice characterized by cosine functions. Note that, unlike the Bessel lattices, the intensity of the elliptic rings in an EPL is not constant; actually the maximum and minimum intensities correspond to the major and minor axes, respectively.

First we address the properties of the stationary solitons supported by the central guiding core of the EPL. We look for solutions of Eq. (1) in the form $\Psi(\mathbf{r},z)=U(\mathbf{r})\exp(i\beta z)$, where $U(\mathbf{r})$ is a real function and β is the longitudinal propagation constant. The soliton profiles depicted in Figs. 1(d)–1(f) were obtained by solving Eq. (1) with the Petviashvili relaxation method [15] starting from a Gaussian ansatz centered at the origin $\mathbf{r}=0$. For small values of β, the solitons have a narrow bell-shaped pattern and concentrate mostly within the elliptic dark spot of the lattice [Fig. 1(d)]. As β increases, the field is wider and covers the first ring producing an elliptic ring-shaped stable soliton [Fig. 1(e)]. For higher values of β, the symmetry breaking instability [16] is developed, and the soliton concentrates on one of the maxima of the first elliptic ring [Fig. 1(f)].

Stationary solitons can also be trapped in the outer rings of the EPL. In Fig. 2 we show the relation between the soliton power $P=\int|U(\mathbf{r})|^2 \mathrm{d}x\mathrm{d}y$ and the propagation constant β for two different points of localization in either the semi-major ($x=4.05$, $y=0$) or the semi-minor ($x=0$, $y=3.9$) axis of the second ring of the EPL. For both cases, we found that to obtain stationary solitons located on the second ring, the Petviashvili relaxation method achieves convergence just when β is restricted to a finite interval of values that in fact reduce as the lattice depth p increases. Applying the Vakhitov–Kolokolov stability criterion [17], namely, $\mathrm{d}P/\mathrm{d}\beta>0$, we predict that all the solitons displayed in Fig. 2 should be stable. We confirmed this prediction by propagating numerous soliton profiles with a split step-Fourier method along hundreds of diffraction lengths.

The most important example of localized self-trapped light modes supported by EPLs is given by stable rotating solitons trapped in the rings of the helical Mathieu lattice. To induce them, we located the centroid of the Gaussian ansatz at the maximum of the second elliptic ring and induce the rotational motion by imprinting an initial transverse momentum $g_\perp$ directed along the tangent of the ring; this can be done by imposing a phase twist $\exp(ig_\perp y)$ on the stationary solutions obtanied previously in the semi-major axis of the second ring. For small values of $g_\perp$ the soliton is still strongly attracted by the local maximum of the elliptic ring and thus oscillates back and forth across this point following an oscillatory trajectory on propagation as shown in Figs. 3(a) and 3(g), where in this case $g_\perp=0.314$.

The rotational motion of the soliton along the elliptic rings is induced by increasing $g_\perp$ until a critical value, g_{rot}. In this case, the soliton gets away from the intensity maximum and undergoes elliptic rotations on propagation as shown in Figs. 3(b) and 3(g), where $g_\perp=0.628$. The dynamics of the rotating solitons arise from the delicate interplay between the attracting force of the particular ring and the initial transverse momentum and power imprinted to the solitons. We performed an extensive set of simulations under different initial conditions and perturbations. To quantify the radiation power, at every propagation step, we calculated the power contained in a circle centered on the soliton whose radius initially encloses 99% of the soliton power at the plane $z=0$. Remarkably, for stable solitons, the enclosed power oscillates but remains conserved. We thus cor-

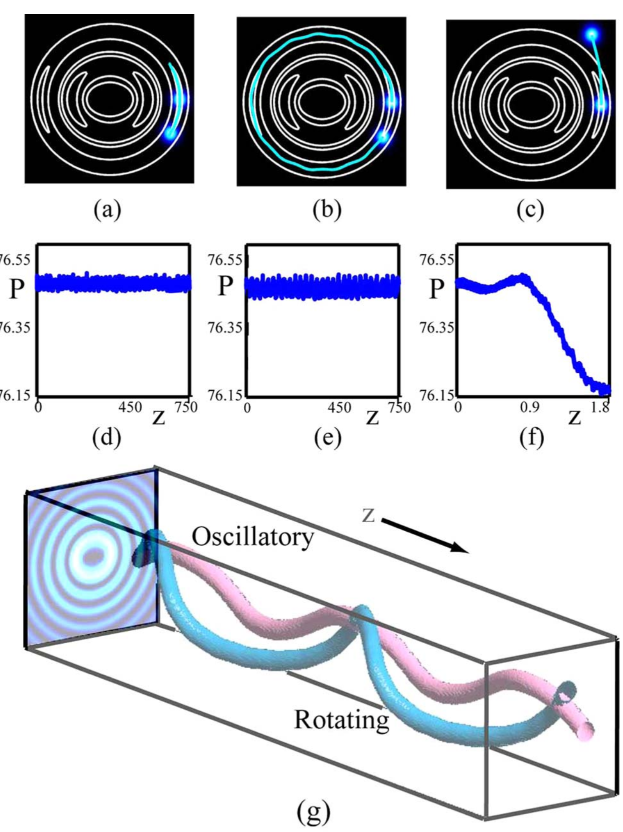

Fig. 3. (Color online) Dynamics of soliton propagation in the EPL with $m=3$ and $\epsilon=1$. In all cases $s=0.05$, $p=4$, and $\beta=10$. (a) Oscillatory motion. (b) Rotational motion. (c) Nontrapped motion. The loss of the power for the soliton propagation for each of these cases is shown in (d), (e), and (f), respectively. (g) Propagation trajectories of the soliton in the EPL for cases (a) and (b). In this example, $g_{\mathrm{rot}}=0.513$ and $g_{\mathrm{out}}=1.53$.

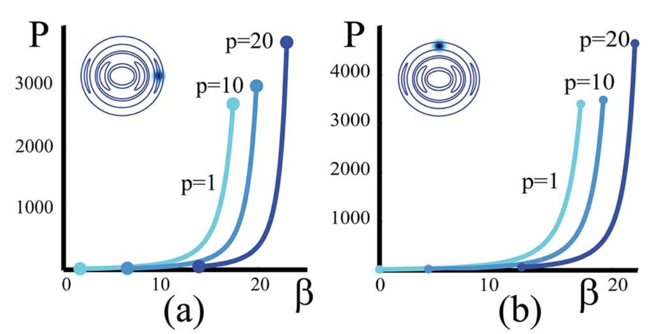

Fig. 2. (Color online) Power of the soliton and their localization into the lattice (inset) versus the propagation constant for different values of lattice depth p for modes localized over (a) the semi-major axis and (b) the semi-minor axis of the second elliptic ring.

roborated that rotating solitons can survive for several tens of elliptic rotations, in spite of the varying modulation of the refractive index in the EPL. If the initial momentum $g_{\perp}$ exceeds a critical value, namely, g_{out}, the soliton leaves the ring where it was initially launched and propagates across the lattice radiating power until it decays. Figure 3 shows the soliton dynamics and the soliton power for the three cases discussed.

Since the refraction index along the rings of the EPL is not azimuthally symmetric, solitons trapped within the elliptic rings increase (decrease) their angular speed as they approach intensity maxima (minima). In Fig. 4, we show the varying rotation rate of the solitons trapped in the EPL and the practically constant rate of the solitons in the Bessel lattice. It is interesting to note that similar elliptic trajectories with varying angular speed have been reported in [13] using trapped spherical polystyrene particles suspended in D_2O. Even though the trapping mechanisms are fundamentally different, in both cases the varying velocity of the trapped particles and solitons is due to the particular modulation of the helical Mathieu beams.

Finally, we remark that a rich variety of interacting scenarios for a collection of stable solitons undergoing elliptic rotation can be obtained, thus featuring unique types of interactions. For example, collisions between solitons launched at different points of the elliptic ring, with identical initial transverse speed and rotating in the same direction, are possible owing to the angular modulation of the ring. These interactions depend heavily on the initial phase difference between each soliton profile. The authors are currently working on a manuscript to show all these results.

In conclusion, we showed that the EPL, with several confocal elliptic rings, supports soliton propagations that are stable in a region of their existence domain by properly adjusting the lattice depth, the ellipticity of the EPL, and the initial power and momentum of the launched fields. Upon propagation, the trajectories of the stable solitons can be stationary, oscillatory, or rotating. Accurate numerical simulations have demonstrated that the soliton can survive, without power radiation, for several hundreds of diffraction lengths and rotations. The possibility of excitation of rotational motion of solitons inside EPL might find direct applications in future soliton circuits. The first controlled soliton rotation in circular ring-shaped photonic lattices by optical induction was demonstrated in [18], opening the possibility to observe experimentally the theoretical results presented in this Letter.

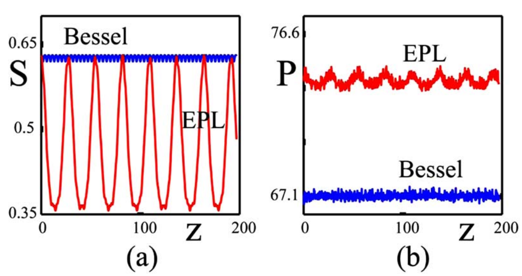

Fig. 4. (Color online) (a) Transverse rotation rate [$S = |\Delta \mathbf{r}|/\Delta z$] of the solitons trapped in an EPL and a Bessel lattice. (b) Enclosed power for soliton trapped in the EPL and the Bessel lattice.

S. Lopez-Aguayo thanks Yuri S. Kivshar and Y. V. Kartashov for useful comments. This work has been supported by Consejo Nacional de Ciencia y Tecnología (grant 82407) and by Tecnológico de Monterrey (grant CAT141).

References

1. D. N. Christodoulides, F. Lederer, and Y. Silberberg, Nature **424**, 817 (2003).
2. J. W. Fleishcer, M. Segev, N. K. Efremidis, and D. N. Christodoulides, Nature **422**, 147 (2003).
3. N. K. Efremidis, S. Sears, D. N. Christodoulides, J. W. Fleischer, and M. Segev, Phys. Rev. E **66**, 046602 (2002).
4. O. Bang and P. D. Miller, Opt. Lett. **21**, 1105 (1996).
5. Y. V. Kartashov, A. S. Zelenina, L. Torner, and V. A. Vysloukh, Opt. Lett. **31**, 238 (2006).
6. Z. Bouchal, Czech. J. Phys. **53**, 537 (2003).
7. S. Chávez-Cerda, J. C. Gutiérrez-Vega, and G. H. C. New, Opt. Lett. **26**, 1803 (2001).
8. M. A. Bandres, J. C. Gutiérrez-Vega, and S. Chávez-Cerda, Opt. Lett. **29**, 44 (2004).
9. Y. V. Kartashov, V. A. Vysloukh, and L. Torner, Phys. Rev. Lett. **93**, 093904 (2004).
10. R. Fischer, D. N. Neshev, S. Lopez-Aguayo, A. S. Desyatnikov, A. A. Sukhorukov, W. Krolikowski, and Y. S. Kivshar, Opt. Express **14**, 2825 (2006).
11. Y. V. Kartashov, A. A. Egorov, V. A. Vysloukh, and L. Torner, Opt. Lett. **31**, 238 (2006).
12. Y. V. Kartashov, V. A. Vysloukh, and L. Torner, Opt. Lett. **33**, 141 (2006).
13. C. Lopez-Mariscal, J. C. Gutiérrez-Vega, G. Milne, and K. Dholakia, Opt. Express **14**, 4182 (2006).
14. Y. Kartashov, V. Vysloukh, and L. Torner, Opt. Express **12**, 2831 (2004).
15. D. E. Pelinovsky and Yu. A. Stepanyants, SIAM (Soc. Ind. Appl. Math.) J. Numer. Anal. **42**, 1110 (2004).
16. Y. S. Kivshar and D. E. Pelinovsky, Phys. Rep. **331**, 117 (2000).
17. A. V. Burvak, Y. S. Kivshar, and S. Trillo, Phys. Rev. Lett. **77**, 5210 (1996).
18. X. Wang, Z. Chen, and P. G. Kevrekidis, Phys. Rev. Lett. **96**, 083904 (2006).